Ingeniería e Investigación
ISSN: 0120-5609
ISSN: 2248-8723
Facultad de Ingeniería, Universidad Nacional de Colombia.

Ruelas-Santoyo, Edgar A.; Vázquez-López, José A.; Yañez-Mendiola, Javier; Baeza-Serrato, Roberto; Jimenez-García, José A.; Sanchez-Márquez, Juan

System for the recognition of wear patterns on microstructures of carbon steels using a multilayer perceptron

Ingeniería e Investigación, vol. 38, no. 1, 2018, January-April, pp. 113-120
Facultad de Ingeniería, Universidad Nacional de Colombia.

DOI: https://doi.org/10.15446/ing.investig.v38n1.60265

DOI: http://dx.doi.org/10.15446/ing.investig.v38n1.60265

System for the recognition of wear patterns on microstructures of carbon steels using a multilayer perceptron

Sistema para el reconocimiento de patrones de desgaste en microestructuras de aceros al carbón utilizando una perceptrón multicapa

Edgar A. Ruelas-Santoyo[1], José A. Vázquez-López[2], Javier Yañez-Mendiola[3], Roberto Baeza-Serrato[4], José A. Jimenez-García[5], and Juan Sanchez-Márquez[6]

ABSTRACT

This paper describes the application of a recognition system wear patterns present in carbon steel, the system classifies the microstructure of the materials which have three conditions throughout life-time in thermoelectric plants. This approach employs the artificial neural network multilayer perceptron in conjunction with the digital image processing to recognize the different physical states of the materials used as conductors in conditions of high temperatures. The studied patterns in the microstructure are spheronization, decarburization and graphitization. The microstructure is revealed from microscope images obtained in the Testing Laboratory Equipment and Materials of the Federal Electricity Commission in Mexico (LAPEM-CFE). The proposed system compared to the human expert, obtained an accuracy of 96.83 % with a shorter analysis time and inspection cost.

Keywords: Artificial Neural Network, digital image processing, material defects.

RESUMEN

Este artículo describe la aplicación de un sistema de reconocimiento de patrones de desgaste presente en aceros al carbón, el sistema clasifica la microestructura de los materiales los cuales presentan tres condiciones a lo largo de su vida útil en plantas termoeléctricas. El enfoque propuesto emplea la red neuronal artificial perceptrón multicapa, en conjunto con el procesamiento digital de imágenes para reconocer los diferentes estados físicos de los materiales utilizados como conductores en condiciones de altas temperaturas. La microestructura de las condiciones estudiadas son esferonización, descarborización y grafitización. La microestructura se revela a partir de imágenes de microscopio obtenidos en el Laboratorio de Pruebas de Equipos y Materiales de la Comisión Federal de Electricidad de México (CFE-LAPEM). El sistema propuesto, en comparación con el humano experto, obtuvo una exactitud promedio del 96.82 % con un menor tiempo de análisis y costo de inspección.

Palabras clave: Red Neuronal Artificial, procesamiento digital de imagen, defectos en material.

Received: September 23rd 2016
Accepted: August 28th 2017

Introduction

Metallography studies microscopically the structure of a metal or an alloy (Newell, 2016). It determines the grain size, form and distribution of various phases and inclusions that have a great effect on the metal mechanical properties. The microstructure reveals the mechanical and thermal treatment of the metal and under a given set of conditions; one can predict the metal behavior. The material exhibits metallographic behavior patterns that are diagnosed by metallographic experts based on the

[1] Industrial Engineering, Ph.D.. CIATEC, Mexico. Affiliation: Technological Institute of Irapuato at Department of Industrial Engineering. Mexico. edruelas@itesi.edu.mx

[2] Industrial Engineering, Ph.D.. CIATEC, Mexico. Affiliation: Technological Institute of Celaya at Department of Industrial Engineering. Mexico. antonio.vazquez@itcelaya.edu.mx

[3] Optics, Ph.D.. CIO, Mexico. Affiliation: Center for Applied Innovation in Competitive Technologies at Department Development of New Talent. Mexico. jyanez@ciatec.mx

[4] Industrial Engineering, Ph.D.. CIATEC, Mexico. Affiliation: University of Guanajuato at Department of Management Technologies Master. Mexico. r.baeza@ugto.mx

[5] Industrial Engineering, PhD.. CIATEC, Mexico. Affiliation: Technological Institute of Celaya at Department of Industrial Engineering. Mexico. alfredo.jimenez@itcelaya.edu.mx

[6] Chemical Engineering, Ph.D.. UG, Mexico. Affiliation: University of Guanajuato at Department of Chemical Engineering. Mexico. ja.sanchez@ugto.mx

How to cite: Ruelas-Santoyo, E. A., Vázquez-López, J. A., Yañez-Mendiola, J., Baeza-Serrato, R., Jimenez-García, J. A., and Sanchez-Márquez, J. A. (2018). System for the recognition of wear patterns on microstructures of carbon steels using a multilayer perceptron. *Ingeniería e Investigación*. 38(1), 113-120. DOI: http://dx.doi.org/10.15446/ing.investig.v38n1.60265

image of the material's microstructure. The quality of the diagnosis to detect the metallographic pattern present in the material depends to a large extent on the experience of the human expert (Barroso, 2014). This paper proposes an alternative solution to make a wear diagnostic system using an Artificial Neural Network (ANN) classification scheme based on a pattern-recognition system employing the multilayer perceptron in conjunction with digital image processing to classify patterns in the image from the metal microstructure. Digital image processing is used first to improve the quality of the image, thus defining an appropriate input signal to the ANN.

Research has been carried out where the benefits of the integration of networks in the field of materials were verified. One of the main activities of artificial neural networks within the area of materials is the estimation. In the work presented by Chokshi (2017), a phase prediction model was developed by means of a multi-layer artificial neural network, the model is used in the experiments carried out on the 22MnB5 steel in order to apply a process called hot stamping with which the microstructures of the material are controlled. The artificial neural network obtained an error of 7,7 % making it a reliable mechanism. In Chakraborty (2017), an artificial neural network model was developed for predicting the phase transformation of steel by austenite, and thus the construction of the continuous cooling transformation diagram. Within the research is used a multi-layer artificial neural network and its weights are defined by a genetic algorithm.

In the research carried out by Jiao (2015), it is demonstrated that the use of a radial-based neural network is capable of analyzing and predicting the electrical resistivity of the aluminum alloy Al-Zn-Mg-Cu experimental data were taken in situ using an optical microscopy, scanning electronics and transmission electronics. The results show that the model is able to predict electrical resistivity with remarkable success reaching a high level of generality. The correlation coefficient between the expected results and the experimental data is 0,9958 and the relative error is 0,33 %.

Another work that relates artificial neural networks and materials science is presented by Powar (2015). In this research, it was proposed to develop a methodology to predict the mechanical properties and microstructure of thermally treated materials, the prediction is done by means of an artificial neural network and the application case was carried out on a shaft made of 30CrMoNiV5-11 steel. The data set for modeling the neural network was generated by studying the microstructural parameters and mechanical properties. In the study, a correlation coefficient (R) of more than 90 % was obtained to predict the mechanical properties and microstructural behavior of the thermally treated steel. In Guo (2016), the ability of the backpropagation artificial neural network to estimate the stress-deformation relationship of the Ti-6Al-4V alloy was demonstrated; experimentation was carried out by thermal compression tests varying the temperature range. Due to reliable performance in tracking and predicting data, the model was used to expand the volume of stress-strain data.

In the investigation developed by Singh (2016), also the effect of the materials due to the temperature is studied, in this work the behavior of hot deformation of the steels with high phosphorus content was defined through thermo-mechanical simulations for temperatures between 750 °C and 1 050 °C. The behavioral estimation was performed through a multi-layered neural network, the inputs of the neural network were: temperature, deformation and strain rate. In the work presented by Dae (2014), the deterioration under the phenomenon of oxidation at a high temperature in Ni-Cr-W-Mo alloys is studied. A database was constructed from cyclic oxidation experiments performed between 400 °C and 1 150 °C of 27 alloys with different Cr, W and Mo contents. The Bayesian neural network technique was used for the modeling of oxidation experiments cyclic. The model shows an accurate prediction of the oxidation property of Ni-Cr-W-Mo alloys (R = 0,999).

An important characteristic of artificial neural networks is the ability to solve tasks of recognition and classification of patterns, an application where this task is solved in the metallographic area is presented by (Hou, 2016), in the research, a system was developed capable of identify the type of corrosion suffered by carbon steel in aqueous media. The types of damages studied are: uniform corrosion, stinging and passivation.

In the investigation presented by Pouraliakbar (2015), an artificial neural network model with feed forward topology and back propagation algorithm was developed to predict the toughness of high strength low alloy steels. The inputs of the neural network included the weight percentage of 15 alloying elements and the tensile test results such as yield strength, ultimate tensile strength and elongation. The model was developed whit 118 different steels from API X52 to X70 grades. The model was validated with 26 steels. The developed model was very accurate and had the great ability for predicting the toughness of pipeline steels. In Pouraliakbar (2015), a neural network with feed-forward topology and back propagation algorithm was used to predict the effects of chemical composition and tensile test parameters on hardness of heat affected zone (HAZ) in X70 pipeline steels. The paper developed by Khalaj (2014), presents results of a research connected with the development of new approach based on the artificial neural network (ANN) of predicting the transformation start temperature of the phase constituents occurring in steels after continuous cooling. The training and testing results in the ANN show a strong potential for prediction of effects of chemical compositions and heat treatments on phase transformation of microalloyed steels. In the research realized by Khalaj (2014), the ultimate tensile strength of steel made using thermomechanically controlled processing has been modeled by means of gene expression programming. To build the model, training and testing using experimental results from 104 specimens were conducted. The training and testing results in gene expression programming models have shown a strong potential for correlating the ultimate tensile strength to yield strength and chemical composition of X70 pipeline steels.

According to the review, it is observed that the use of artificial neural networks is viable as a method of estimation and recognition of the deterioration present in the materials. The proposed work uses the artificial neural network multilayer preceptron as a mechanism for recognition and classification of metallographic patterns, and incorporates digital image processing as a tool that aims to generate detailed input signals to the artificial neural network.

The study presented in this article combines the use of neural networks with digital image processing where the network is trained by the histogram of an image that has been previously segmented and binarized; this procedure provides efficient results in the classification-recognition of carbon steel states (decarburization, graphitization and spheronization) that, to the best knowledge of the authors, have not been addressed from the viewpoint of Artificial Intelligence. The maintenance program within a power plant includes the health monitoring of the metal structures including the steam and water conducts that work at high pressures and temperatures. These conducts come from the steam turbine and generator as it is illustrated in Figure 1. Routinely, metal samples are taken and stored in a database with the purpose of being analyzed by a material expert with associated high costs.

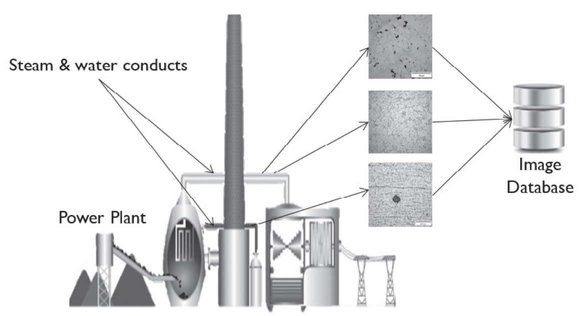

Figure 1. Power plant generation and metal sample collection.
Source: Authors

The development of the wear pattern recognition system rises from the need to corroborate the diagnostic made by a metallographic expert and also to automate the process since the human expert may not be available or there can be a shortage of such highly qualified specialist. The importance of the system lies on the recommendation of whether the material is still in working conditions or needs to be replaced. In current practice within the power plant, a failure to diagnose correctly the state of the material can lead to high costs in the case of early replacement or potentially deadly consequences if the defective material continues in operation.

The material under study is the carbon steel grade A210 C, because it is one of the most used for the construction of conductors of water and steam under high temperatures in thermoelectric plants in Mexico materials. The Contact with high temperatures causes damage to the material throughout its useful life and transforms its microstructure over time. According to ASTM 210-02 the steel has the chemical specifications described in Table 1.

Table 1. Steel Composition

Carbon (C)	Manganese (Mn)	Phosphorus (P)	Sulfur (S)	Silicon (Si)
0,27 max	0,29-1,06	0,035 max	0,035	0,10 min

Source: Norm ASTM 210-02

The proposed wear recognition system is intended to facilitate the plant condition monitoring in the steam and water metal conducts. Currently, several samples are taken from the conducts and stored in a database to later on, be analysed by a failure specialist. The basic idea is to use this image knowledge base to train an ANN in order to learn to recognize and classify the three principal condition states avoiding the requirement of a human expert. This procedure is illustrated in Figure 2.

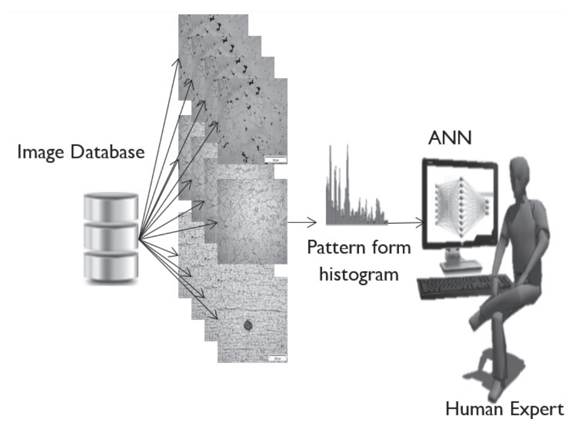

Figure 2. Wear pattern recognition system.
Source: Authors

Digital image processing

The process starts obtaining a metallographic image consisting of consecutive operations. The first operation is to cut the affected material in order to remove small sections to reveal information about the cause and the range of the damage. The next step is the manufacture of a test tube with epoxy resin, sanded and polished with silicon carbide solution to get a mirror finish. Next, a Nital solution with concentration of 4 % is applied for five seconds to disclose the microstructure. Finally, the specimen is observed by the human expert using an inverted metallographic microscope (Olympus-GX71) and an image analyzer (Analysis five). Once the image sample is taken this image can be stored and transmitted for further processing. The techniques of digital image processing are used in order to improve the visual appearance for an observer and conveniently prepare photographic content in the face of machine perception; in this case, the artificial neural network. A flowchart indicating operations in the process of extraction and preprocessing of metallographic images is illustrated in Figure 3.

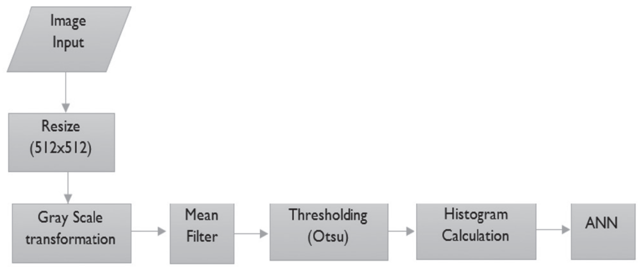

Figure 3. Digital image processing.
Source: Authors

This is the part of the image pre-processing stage for the input image to lower the spatial resolution. After trying different spatial resolutions such as: [1024 × 1024] [512 × 512] and [256 × 256], it was concluded that best results were achieved with [512 × 512] pixels defining also the length of the histogram. The histogram is the input to the neural network and if it is obtained from higher resolution images then the computing efficiency of the neural network can be compromised. On the other hand, having a lower resolution can result in a misclassification. In Figure 4, the image resizing is illustrated using patterns related to graphitization and decarburization.

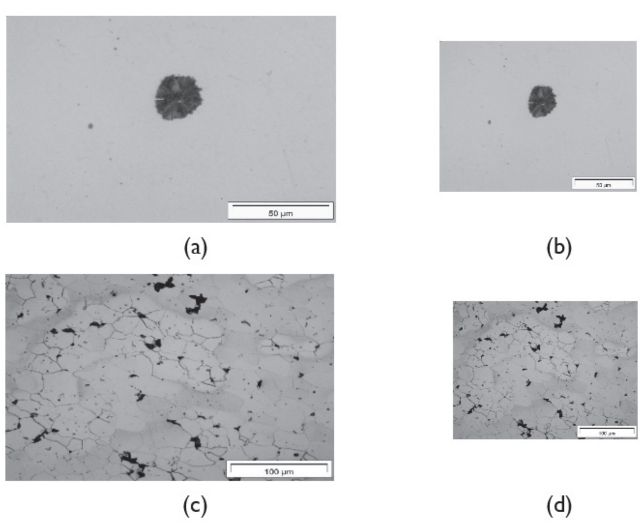

Figure 4. Image Resizing. (a) Original graphitization image [3072 × 4080 pixels]. (b) Resized image [512 × 512 pixels]. (c) Original decarburization image [602 × 800]. (d) Resized image (c) [512 × 512 pixels].
Source: Authors

Image filtering

Filtering is applied to enhance or attenuate spatial detail in order to enhance the visual interpretation or facilitate further processing and it is one of the techniques involved in image enhancement. A low-pass median filter is used employing a [3x3] mask, which basically replaces the central pixel value to the value determined by the multiplication. In Figure 5 and Figure 6, the result of the median filtering is shown in the metallographic images with their respective intensity histogram, calculated from the accumulated sum in the image columns.

It is important to make the difference between the histogram used as input signal to the ANN and a histogram representing the intensity levels. The first is constructed from the sum of the columns of the matrix that makes up the image digitally processed. The second is a graph representing the levels of color intensity in a certain image, concerning the number of pixels present in the image with each color intensity.

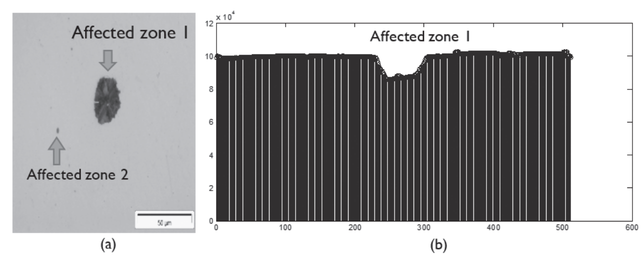

Figure 5. Filtered graphitization image and histogram. (a) Filtered image (b) Histogram.
Source: Authors

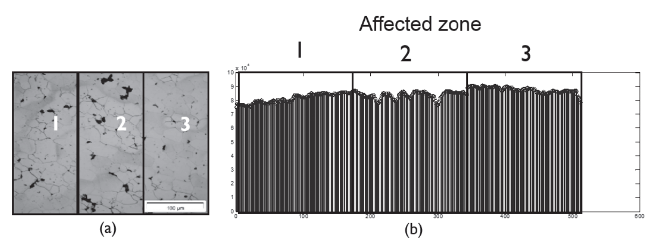

Figure 6. Filtered decarburation image and histogram. (a) Filtered image (b) Histogram.
Source: Authors

The intensity histogram after applying the median filter to the image for graphitization does not show in detail the affected areas. For instance, through inspection we can observe that the affected zone 2 does not appear in the given histogram. See Figure 5(a) and 5(b). The pattern behavior for decarburization in the affected zone 1 (Figure 6(a)) does not show in a clear way inside the generated histogram from the metallographic image. See Figure 6(b). Considering these results, it is not possible to provide an adequate input signal to the ANN for the classifying-recognition task, therefore image segmentation is recommended.

Image Segmentation

It is a stage of digital image processing that locates and separates different areas within an image based on a defined intensity threshold. This step allows the expert to determine the presence of any abnormal element. There are several methods to appropriately select a threshold.

However, some of them do not work well when working with real-world images due to the presence of noise and varying lighting. Considering this, we decided to borrow some ideas from Otsu's method (Wakaf, 2016) to automatically perform histogram shape-based image thresholding, reducing a gray level image to a binary image. The algorithm assumes that the image to be thresholded contains two classes of pixels (e.g. foreground and background) then calculates the optimum threshold separating those two classes so that their combined intra-class variance is minimal. Let us define the global and intra-class variances as in Equation (1).

$$\sigma_G^2 = \sum_{i=0}^{L-1} (i - m_G)^2 \mathrm{P}_i; \; \sigma_B^2 = \mathrm{P}_1 (m_1 - m_G)^2 + \mathrm{P}_2 (m_2 - m_G)^2 \quad (1)$$

Respectively, where L is the number of gray levels (typically 256), m_G is the average gray level in the image and P_i is the probability of the i_{th} gray level in the image. The probabilities P_1 and P_2 of the two potential classes C_1 and C_2 are defined respectively as $\mathrm{P}_1(\mathrm{k}) = \sum_{i=0}^{k} \mathrm{Pi}$ and $\mathrm{P}_2(\mathrm{k}) = 1 - \mathrm{P}_1(\mathrm{k})$ with $0 < \mathrm{k} < \mathrm{L} - 1$. The average probabilities m_1 and m_2 of C_1 and C_2 are defined respectively as $\mathrm{m}_1(\mathrm{k}) = \frac{1}{\mathrm{P}_1(\mathrm{k})} \sum_{i=0}^{k} \mathrm{iP}_i$ and $\mathrm{m}_2(\mathrm{k}) = \frac{1}{\mathrm{P}_2(\mathrm{k})} \sum_{i=k+1}^{L-1} \mathrm{iP}_i$.

Note that the optimal classes C_1 and C_2 are separated by the k_{th} gray level value that makes maximal. The relationship between global and intra-class variances is given by $\eta(\mathrm{k}) = \sigma_B^2(\mathrm{k}) / \sigma_G^2$. This means that the intra-class variability must be evaluated for every gray level as $\sigma_B^2(\mathrm{k}) = (\mathrm{m_G P_1(k)} - \mathrm{m(k)})^2 / \mathrm{P_1(k)}(1 - \mathrm{P_1(k)})$, with $\mathrm{m(k)}$ being the cumulative average probability up to the k_{th} gray level.

The optimal threshold is then defined as k satisfying. Equation (2).

$$\sigma_B^2(k) = \max\left(\sigma_B^2(k)\right) \quad (2)$$

For the total number of changes in light source intensity, the criterion is shown in Equation (3).

$$\eta_b(n) = \frac{\sigma_B^2(k^*, n)}{\sigma_G^2(n)}, \; 1 < n < N \quad (3)$$

is recorded for every n_{th} intensity variation, where N is the number of variations. The n_{th}^* image maximizing the criterion is then selected using the equation $\eta_b(n^*) = \max(\eta_b(n))$. Finally, the optimal threshold k^* is used to segment the selected image, (Gonzalez, 2009). Using this approach, the affected zones are clearly visible as it is shown in Figure 7, where the graphitization pattern and decarburization pattern are shown after binarization and segmentation.

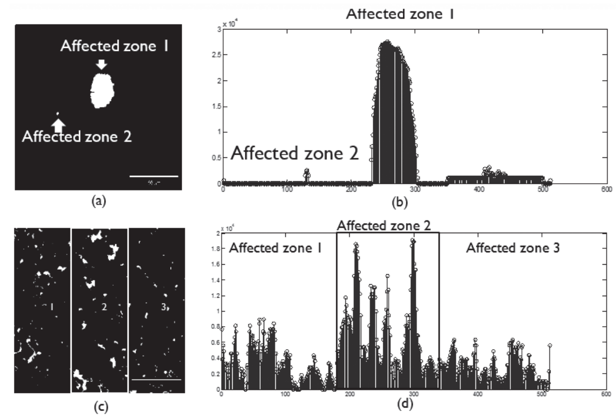

Figure 7. Image Segmentation. (a) Graphitization pattern. (b) Histogram (c) Decarburization pattern. (d) Histogram.
Source: Authors

Neural Network

An artificial neural network is a massively parallel processor which consists of simple processing units that have a natural property to store experimental knowledge, making it viable for use. The neural network resembles the brain in two respects:

i. Knowledge is acquired by the network from its environment through a learning process.

ii. The strength of the connections between neurons, known as synaptic weights are used to store knowledge.

A neural network architecture is the organization and arrangement of neurons in the network forming layers or groups of neurons. The basic parameters are: number of layers, number of neurons per layer, degree of connectivity and type of connection between neurons.

Multilayer networks

Multilayer neural networks are formed with a group of simple cascading layers. The output of one layer is the input of the next layer. It is known that multilayer networks have superior learning performance compared to networks of a single layer. Since these networks have several layers, the connections between neurons can be feed forward type (forward connection) or feedback type (back connection). Feed forward networks are particularly useful in applications for pattern recognition or classification. The Figure 8, shows the general structure of these types of networks. Figure and nomenclature are taken from (Haykin, 2009).

The input to the network is the vector **p** whose length is equal to R, **W** is the weight matrix with dimensions SxR. **a** and **b** are vectors of length S which represents the number of neurons in the network.

The ability of the multilayer perceptron network to learn from a set of examples, to approximate nonlinear relationships, filter noise in the data, etc. makes it a suitable model to address real problems and appropriate tools as universal approximators (Gamarra, *et al.*, 2013). The design of the network architecture involves defining the activation function, the number of neurons and the number of layers in the network. Choosing the activation function is usually done based on the required smoothness for the output signal in the hidden layers, though its election does not affect the ability of the network to solve the problem (Benitez, 2014).

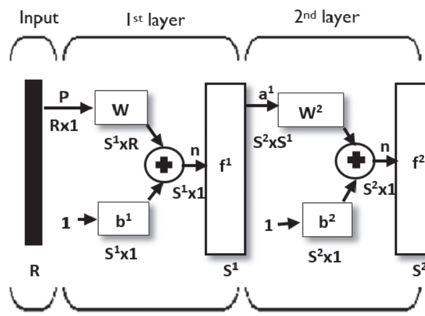

$$\mathbf{a}^1 = \mathbf{f}^1(\mathbf{W}^1\mathbf{p} + \mathbf{b}^1) \quad \mathbf{a}^2 = \mathbf{f}^2(\mathbf{W}^2\mathbf{a}^1 + \mathbf{b}^2)$$

$$\mathbf{a}^2 = \mathbf{f}^2(\mathbf{W}^2\mathbf{f}^1(\mathbf{W}^1\mathbf{p} + \mathbf{b}^1) + \mathbf{b}^2$$

Figure 8. General structure of a multilayer neural network.
Source: Haykin, 2009

As for the number of neurons and layers, some of these parameters are given by the problem and others should be chosen and defined by the designer. The number of neurons in the input layer and in the output is defined by the number of input and output variables which characterize the problem. The number of hidden layers and number of neurons in these layers must be chosen by the designer. There is not a method to determine the optimal number of hidden layers and neurons to solve a given problem. The use of the ANN in the wear pattern recognition system is described by a flow chart given in Figure 9.

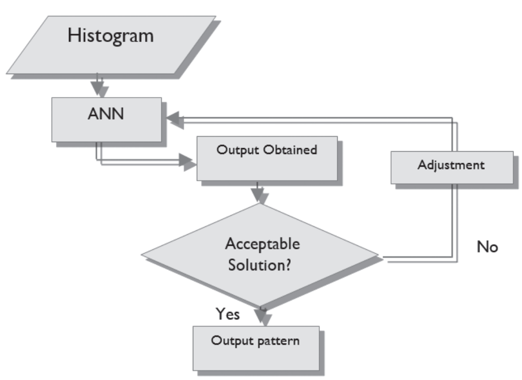

Figure 9. Classification-Recognition Process.
Source: Authors

The adjustment relates to the action of modifying parameters that make up the topology of the ANN to achieve a combination of parameters that yields an acceptable solution to the classification presented to the network. These parameters are: number of neurons in the hidden layer, learning rate, training time and allowed error. See Table 4.

Experimental methodology

The study case for this research was carried out in the Laboratory of Equipment and Materials Testing (LAPEM) of the Federal Electricity Commission (CFE). Typical spheronization (a), decarburization (b) and graphitization (c) image patterns are presented in Figure 10.

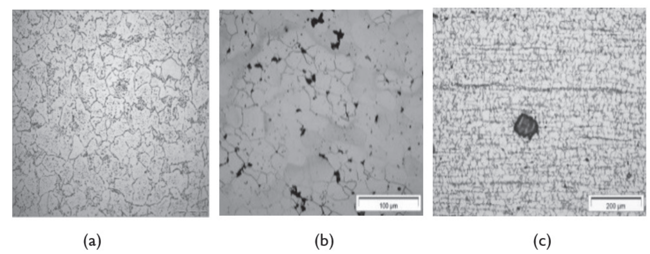

Figure 10. Metallographic patterns studied.
Source: Authors

The pattern set employed to train and test the neural network was a database of four hundred and sixteen metallographic images affected by patterns previously recognized and identified by experts at LAPEM. The training matrix was generated from the process shown in Figure 3, defining a final input matrix $[124 \times 512]$ incorporated to the neural multilayer perceptron network which was defined according to the number of images selected for the training phase (124) leaving (292) for the testing phase. The dimension of the training and testing matrix are shown in Table 2.

Table 2. Training and Testing matrix

Pattern	Training	Testing
Spheronization	56×512	122×512
Decarburization	29×512	84×512
Graphitization	39×512	86×512

Source: Authors

The activation function in the architecture of the ANN is a hyperbolic tangent, the value of (-1) to spheronization, (0) Decarburization and (1) graphitization, are assigned. The topologies of ANN's proposals in Table 3, are adequately conform the 124 target values corresponding to metallographic pattern in the training phase, which is why was resorted to a statistical parameter as the root mean square error (MSE) to determine which topology should be selected and then used in the test phase with the remaining 139 images. The values of the ANN were rounded to the closest integer and then compared against the target values.

Table 3. Proposed Topologies

Topology	Number of neurons in the hidden layer	Learning rate	Allowed Error	Epochs	Correlation Coefficient. R	Mean squared error. MSE
1	26	0,01	1e-5	3 000	0,99991	0,000789541
2	27	0,01	1e-5	5 000	0,99989	0,001139443
3	26	0,005	1e-5	5 000	0,99915	0,004998984
4	28	0,01	1e-5	3 000	0,99989	0,006498906
5	28	0,005	1e-5	5 000	0,99956	0,011839077
6	27	0,005	1e-5	3 000	0,99919	0,034691897

Source: Authors

Results

In order to verify the proper operation of the network and the ability to solve the task of wear pattern detection, a validation phase was developed introducing 292 new images of spheroidization, decarburization and graphitization patterns for classification and recognition. The metallographic images were previously recognized and identified by human experts (targets). The results for the validation phase in each of the topologies developed with the parameters described in Table 3 are given in the Figure 11. The code was developed in the Matlab® 2015. It is possible to validate a correct classification-recognition through the following indicators: sensitivity Equation (4), specificity Equation (5) and accuracy Equation (6). The probability of not making a type I error, (1-α), is known as test efficiency, equivalent to specificity. The probability of not making a type II error, (1-β), is known as the power of the test, equivalent to sensitivity. The degree of accuracy of a test is defined as the percentage of cases in which the result is correct.

$$Sensitivity = \frac{VP}{VP + FN} \tag{4}$$

$$Specificity = \frac{VN}{VN + FP} \tag{5}$$

$$Accuracy = \frac{VP + VN}{VN + FP + VP + FN} \tag{6}$$

Where: VP - True-Positive; FN - False-Negative; VN - True-Negative; FP - False-Positive

From the indicators of sensitivity, specificity and accuracy it was demonstrated that using the histogram generated from the digital processing of metallographic image, generates a signal efficient entry to the ANN and thus be able to perform the classification task-recognition through architecture presented in Table 4. The topology of the selected artificial neural network was the number 1.

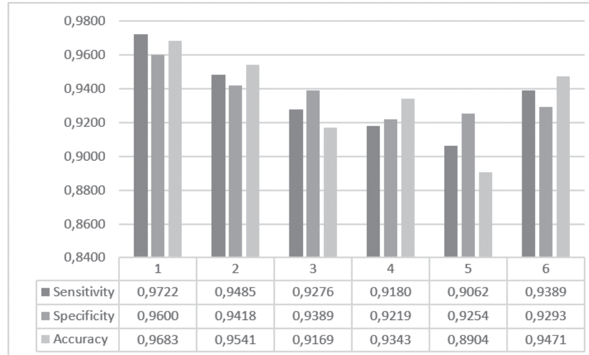

Figure 11. Results of the developed topologies of neural networks.
Source: Authors

Table 4. Topology of the selected artificial neural network

Parameter	Value
Number of hidden layers	1
Number of neurons in the output layer	1
Number of hidden layers	1
Number of neurons in the hidden layer	26
Activation function in the hidden and output layer	hyperbolic tangent
Display during training	50
Learning rate	0,01
Error function value to reach	1e-5
Maximum number of times	3 000
Type training	Conjugate gradient climbing

Source: Authors

The experimental results were obtained using a computer with AMD A10 Processor @3.7 GHz with 16 GB RAM. The time average to reach the allowed error during the learning stage was 31s.

Conclusions

A novel approach to address the problem for structure health monitoring in power plants has been proposed. The methodology involves the use of image information coming from intensity histograms to train an artificial neural network (ANN) to automate the detection of three wear metal states (spheronization, decarburization and graphitization). Obtained results revealed the feasibility of using the system in an automated process to reduce the vast amount of data that a failure expert would have to analyze.

The result of this research will be useful to generate or to confirm a diagnostic accomplished by an expert which is necessary to determine the causes of material failure, maintenance periods or parts replacement. The methodology presented is efficient according to indicators of sensitivity (97,22 %), specificity (96 %) and average accuracy (96,83 %). An important aspect is due to the fact that the digital image becomes a wear pattern using the histogram of intensity to produce a pattern input to the ANN. Another important point is that in order to increase the robustness of the segmentation process in different lighting conditions, the Otsu's method was employed to select the best threshold value. Under the above it is possible to think of establishing this procedure in companies that require analysis of materials in use and do not have an expert immediately.

References

Barroso, S., & Ibáñez, J. (2014). *Introducción al conocimiento de materiales*. Madrid, Spain: UNED. ISBN: 8436268598, 9788436268591.

Benitez, R., Escudero, G., Kanaan S., & Rodó, D. (2014). *Inteligencia artificial avanzada*. Barcelona, Spain: UOC. ISBN: 8490643210, 9788490643211.

Chakraborty, S., Chattopadhyay, P., Ghosh, S., & Datta, S. (2017). *Incorporation of prior knowledge in neural network model for continuous cooling of steel using genetic algorithm*. Applied Soft Computing, 58, 297-306. DOI: https://doi.org/10.1016/j.asoc.2017.05.001

Chokshi, P., Dashwood, R., & Hughes, J. (2017). *Artificial Neural Network (ANN) based microstructural prediction model for 22MnB5 boron steel during tailored hot stamping*. Computers & Structures, 190, 162-172. DOI: https://doi.org/10.1016/j.compstruc.2017.05.015

Dae, Y., Seo, S., Jeong, H., Kim, I., & Yoo, Y. (2014). *Modelling high temperature oxidation behaviour of Ni–Cr–W–Mo alloys with Bayesian neural network*. Journal of Alloys and Compounds, 587, 105-112.
DOI: http://doi.org/10.1016/j.jallcom.2013.10.138

Gamarra, M., & Quintero, C. (2013). *Using genetic algorithm feature selection in neural classification systems for image pattern recognition*. Ingeniería e Investigación, 33 (1), 52-58. Retrieved from: https://revistas.unal.edu.co/index.php/ingeinv/article/view/37667/41820

Gonzalez, R., Woods R., & Eddins, S. (2009). *Digital Image Processing Using Matlab*. 2nd. Ed.. United States of America: Gatesmark Publishing. ISBN: 978-0-9820854-0-0.

Guo, Q., Hai, W., & Zhen, Z. (2016). *Construction of processing maps based on expanded data by BP-ANN and identification of optimal deforming parameters for Ti-6Al-4V alloy*. International Journal of Precision Engineering and Manufacturing, 17(2), 171–180.
DOI: https://doi.org/10.1007/s12541-016-0022-z

Haykin, S. (2009). *Neural Networks and Learning Machin*. 3rd. Ed.. New Jersey, United States of America: Pearson Prentice Hall. ISBN-10: 0-13-147139-2

Hou, Y., Aldrich, C., Lepkova, K., Machuca, L., & Kinsella, B. (2016). *Monitoring of carbon steel corrosion by use of electrochemical noise and recurrence quantification analysis*. Corrosion Science, 112, 63-72.
DOI: https://doi.org/10.1016/j.corsci.2016.07.009

Jiao, L., Hong, L., De, L., & Wu, Y. (2015). *Application of novel physical picture based on artificial neural networks to predict microstructure evolution of Al–Zn–Mg–Cu alloy during solid solution process*. Transactions of Nonferrous Metals Society of China, 25(3), 944-953.
DOI: https://doi.org/10.1016/S1003-6326(15)63683-4

Khalaj, G., & Khalaj, M. (2013). *Modeling the correlation between yield strength, chemical composition and ultimate tensile strength of X70 pipeline steels by means of gene expression programming*. International Journal of Materials Research, 104 (7), 697-702.
DOI: https://doi.org/10.3139/146.110910

Khalaj, G., Nazari, A., Yoozbashizadeh, H., Khodabandeh, A., & Jahazi, M. (2014). *ANN model to predict the effects of composition and heat treatment parameters on transformation start temperature of microalloyed steels*. Neural Computing and Applications, 24(2), 301- 308.
DOI: https://doi.org/10.1007/s00521-012-1233-6

Newell, J. (2016). *Ciencia de materiales aplicaciones en ingeniería*. 1st. Ed.. Distrito Federal, México: Alfaomega Grupo Editor. ISBN: 6077073113, 9786077073116.

Pouraliakbar, H., Khalaj, G., Jandaghi, M., & Khalaj, M. (2015). *Study on the correlation of toughness with chemical composition and tensile test results in microalloyed API pipeline steels*. Journal of Mining and Metallurgy, Section B: Metallurgy, 51(2), 173- 178.
DOI: 10.2298/JMMB140525025P

Pouraliakbar, H., Khalaj, M., Nazerfakhari, M., & Khalaj, G. (2015). *Artificial Neural Networks for Hardness Prediction of HAZ with Chemical Composition and Tensile Test of X70 Pipeline Steels*. Journal of Iron and Steel Research International, 22(5), 446-450.
DOI: https://doi.org/10.1016/S1006-706X(15)30025-X

Powar, A., & Date, P. (2015). *Modeling of microstructure and mechanical properties of heat treated components by using Artificial Neural Network*. Materials Science and Engineering, 628, 89-97.
DOI: https://doi.org/10.1016/j.msea.2015.01.044

Singh, K., Rajput, K., & Mehta, Y. (2016). *Modeling of the hot deformation behavior of a high phosphorus steel using artificial neural networks*. Materials Discovery, 6, 1-8. DOI: https://doi.org/10.1016/j.md.2017.03.001

Wakaf, Z., & Jalab, H., (2016). *Defect detection based on extreme edge of defective region histogram*. Journal of King Saud University - Computer and Information Sciences, 30(1), 33-40.
DOI: https://doi.org/10.1016/j.jksuci.2016.11.001